

## Protein dynamics modulated electron transfer kinetics in early stage photosynthesis

Prasanta Kundu and Arti Dua

Citation: *J. Chem. Phys.* **138**, 045104 (2013); doi: 10.1063/1.4789346

View online: <http://dx.doi.org/10.1063/1.4789346>

View Table of Contents: <http://jcp.aip.org/resource/1/JCPSA6/v138/i4>

Published by the [American Institute of Physics](#).

---

### Additional information on *J. Chem. Phys.*

Journal Homepage: <http://jcp.aip.org/>

Journal Information: [http://jcp.aip.org/about/about\\_the\\_journal](http://jcp.aip.org/about/about_the_journal)

Top downloads: [http://jcp.aip.org/features/most\\_downloaded](http://jcp.aip.org/features/most_downloaded)

Information for Authors: <http://jcp.aip.org/authors>

## ADVERTISEMENT

# Instruments for advanced science

### Gas Analysis



- dynamic measurement of reaction gas streams
- catalysis and thermal analysis
- molecular beam studies
- dissolved species probes
- fermentation, environmental and ecological studies

### Surface Science



- UHV TPD
- SIMS
- end point detection in ion beam etch
- elemental imaging - surface mapping

### Plasma Diagnostics



- plasma source characterization
- etch and deposition process
- reaction kinetic studies
- analysis of neutral and radical species

### Vacuum Analysis



- partial pressure measurement and control of process gases
- reactive sputter process control
- vacuum diagnostics
- vacuum coating process monitoring

contact Hiden Analytical for further details

**HIDEN**  
ANALYTICAL

[info@hideninc.com](mailto:info@hideninc.com)  
[www.HidenAnalytical.com](http://www.HidenAnalytical.com)

CLICK to view our product catalogue 

# Protein dynamics modulated electron transfer kinetics in early stage photosynthesis

Prasanta Kundu and Arti Dua

Department of Chemistry, Indian Institute of Technology, Madras, Chennai 600036, India

(Received 13 October 2012; accepted 9 January 2013; published online 31 January 2013)

A recent experiment has probed the electron transfer kinetics in the early stage of photosynthesis in *Rhodobacter sphaeroides* for the reaction center of wild type and different mutants [Science **316**, 747 (2007)]. By monitoring the changes in the transient absorption of the donor-acceptor pair at 280 and 930 nm, both of which show non-exponential temporal decay, the experiment has provided a strong evidence that the initial electron transfer kinetics is modulated by the dynamics of protein backbone. In this work, we present a model where the electron transfer kinetics of the donor-acceptor pair is described along the reaction coordinate associated with the distance fluctuations in a protein backbone. The stochastic evolution of the reaction coordinate is described in terms of a non-Markovian generalized Langevin equation with a memory kernel and Gaussian colored noise, both of which are completely described in terms of the microscopics of the protein normal modes. This model provides excellent fits to the transient absorption signals at 280 and 930 nm associated with protein distance fluctuations and protein dynamics modulated electron transfer reaction, respectively. In contrast to previous models, the present work explains the microscopic origins of the non-exponential decay of the transient absorption curve at 280 nm in terms of multiple time scales of relaxation of the protein normal modes. Dynamic disorder in the reaction pathway due to protein conformational fluctuations which occur on time scales slower than or comparable to the electron transfer kinetics explains the microscopic origin of the non-exponential nature of the transient absorption decay at 930 nm. The theoretical estimates for the relative driving force for five different mutants are in close agreement with the experimental estimates obtained using electrochemical measurements. © 2013 American Institute of Physics. [<http://dx.doi.org/10.1063/1.4789346>]

## I. INTRODUCTION

The early stage of photosynthesis involves an electron transfer reaction from an excited donor to a neighbouring acceptor in an environment of protein matrix. In the case of photosynthetic bacteria *Rhodobacter sphaeroides*, the donor is a special pair of bacteriochlorophylls, which on photoexcitation transfers an electron to a pheophytin to form a charge separated species in picoseconds. In a recent experiment by Wang *et al.*,<sup>1</sup> the reaction center of the wild type and different mutants of *Rhodobacter sphaeroides* was probed by monitoring the changes in the transient absorption of the donor-acceptor pair at 930 and 280 nm. While the signal at 930 nm tracked the kinetics of electron transfer reaction from donor to acceptor, the signal at 280 nm was sensitive to protein conformational dynamics. Interestingly, in an interval of around 1–200 ps, the wild type and mutants showed different temporal decay for the transient absorption at 930 nm. In the same time interval, however, the temporal decay of the transient absorption at 280 nm for different mutants was all the same resulting in data collapse. In spite of these differences, a common feature of both the profiles was the non-exponential temporal decay profiles. The invariance of the 280 nm signal to different mutants in the reaction center provided a strong experimental evidence that protein conformational dynamics occurs on timescales slower than the electron transfer kinetics, implying

that the former effectively modulates the kinetics of electron transfer in the early stages of photosynthesis.

In order to fit the experimental data for the transient absorption curves at 930 and 280 nm, Wang *et al.* used the Sumi-Marcus model of electron transfer<sup>2,3</sup> to calculate the survival probability of excited donor state. The survival probability, among other parameters, depended on a protein relaxation function,  $C_p(t)$ , and the free energy of a protein backbone,  $V_p(x)$ , where  $x$  is the reaction coordinate associated with protein dynamics. However, since the details of protein conformational dynamics were not included in the model,  $C_p(t)$  was considered as an unknown function, the empirical form of which was obtained by fitting a tri-exponential function to the experimental data at 280 nm which yielded three relaxation times. Also,  $V_p(x)$  was assumed to be a harmonic potential. Keeping all other parameter fixed, the same three relaxation times could provide excellent fit to the experimental data at 930 nm for all the different types of mutants in the reaction center by merely changing the driving force,  $\Delta G^0$ , the free energy difference between the donor and acceptor. However, since the protein conformational fluctuations were not included in the model, the microscopic basis for the tri-exponential form of the empirical function,  $C_p(t)$ , and the harmonic nature of the potential  $V_p(x)$ —two key quantities which were crucial to fit the experimental data—is not clear.

To include the effects of protein conformational fluctuations, a recent work<sup>4</sup> models the inter-segment distance fluctuations of a protein by considering a particle in a harmonic potential driven by the fractional Gaussian noise.<sup>5</sup> In this one-dimensional generalized Langevin equation description, the complicated dynamics of protein is included in the memory kernel which depends on the fractional Gaussian noise through the Hurst index  $H$ . Also,  $C_p(t)$  is identified with the time correlation of the inter-segment distance fluctuations of a protein, the form of which is not empirical but can be calculated within the model. Although the agreement between the theory and experimental data for the transient absorption signal at 930 nm is good, the fitting for different mutants in the reaction center has been obtained by varying both  $\Delta G^0$ , the driving force of the reaction and  $\tau$ , the protein relaxation time. The variation of  $\tau$  for different mutants, however, cannot explain data collapse of the transient absorption curves at 280 nm which occurs because protein conformational dynamics is invariant in different mutants. Moreover, no microscopic basis for the memory kernel and the choice of noise, both of which depend on the Hurst index  $H$ , can be provided within the model. In particular, a good fit to the experimental data has been obtained by taking  $H = 3/4$ . From the microscopic point of view, it is not clear why this special value of the Hurst index is successful in reproducing the experimental results at 930 nm.

In this work, we present a model where the electron transfer kinetics of the donor-acceptor pair is described along the reaction coordinate associated with the distance fluctuations in a protein backbone. The stochastic evolution of the reaction coordinate is described in terms of a non-Markovian generalized Langevin equation with a memory kernel and Gaussian colored noise, both of which are completely described in terms of the microscopics of the protein normal modes.<sup>6</sup> This model, apart from providing excellent fits to the experimental data by merely changing the driving force of the electron transfer reaction for different mutants relative to the wild type, explains the microscopic basis for the multiexponential form of  $C_p(t)$  in terms of the multiple time scales of relaxation of protein normal modes and the harmonic nature of the potential in terms of the conformational entropy due to chain connectivity. The microscopic origin of  $H = 3/4$  dependence of the fractional Gaussian noise can also be explained in terms of the non-Markovian distance fluctuations<sup>6</sup> of a protein backbone resulting in a  $t^{-1/2}$  power law decay of the friction kernel observed experimentally.<sup>7</sup> Moreover, the theoretical estimates for the relative driving force for five different mutants are found to be in close agreement with the experimental estimates obtained using electrochemical measurements.<sup>1,8</sup>

The paper is organized as follows. In Sec. II, the key steps involved in the electron transfer reactions modulated by protein conformational dynamics are presented. The evaluation of  $C(t)$  [which is similar to  $C_p(t)$  in Ref. 1] and the survival probability  $S(t)$  of excited donor state are also presented in Sec. II. The comparison of the theoretical results with experimental data is presented in Sec. III followed by summary and conclusions in Sec. IV. The details of the calculation are presented in Appendices A–D.

## II. THE ELECTRON TRANSFER REACTION AND PROTEIN CONFORMATIONAL FLUCTUATIONS

In the early stage of photosynthesis, slow protein relaxation modulates the fast electron transfer kinetics from the excited donor to the acceptor. This slow relaxation is associated with the multiple time scales of relaxation of the normal modes of proteins as a result of which protein conformational fluctuations decay on time scales longer than or comparable to the time scales of the electron transfer reaction leading to dynamic disorder<sup>9</sup> in the reaction pathway. Starting from a Markovian model of protein normal modes relaxation, the slow conformational dynamics of protein backbone can be effectively described by a non-Markovian dynamics of end-to-end distance fluctuations of a protein,  $R(t)$ .<sup>6</sup>

If the electron transfer reaction from the excited donor to acceptor is assumed to follow the first-order kinetics, then the time evolution of the probability density of the electron donor state along a reaction coordinate  $R(t)$ , which evolves stochastically in time, is given by<sup>4</sup>

$$\frac{dP(t)}{dt} = -k(R(t))P(t), \quad (1)$$

where as a result of dynamic disorder the rate constant of the electron transfer reaction depends on the reaction coordinate,  $R(t)$ . The latter is associated with the end-to-end distance fluctuations in a protein backbone, indicating that protein conformational fluctuations which act on the time scales slower than or comparable to the electron transfer reaction, effectively modulate the electron transfer kinetics. The expression for  $k(R)$  is given by

$$k(R) = \left( \frac{J^2}{\hbar} \sqrt{\frac{\pi}{\lambda_f k_B T}} \right) \exp[-(\mu - \gamma R)^2], \quad (2)$$

which can be obtained by considering the fast and slow coordinates of potential energy surfaces of reactants and products<sup>1,2</sup> in terms of the effective bond distance and end-to-end distance fluctuations of the protein backbone, respectively. The details are provided in Appendix A. In the above expression,  $R$  represents the reaction coordinate associated with the end-to-end distance of a protein backbone. Also,  $J$  is electronic coupling matrix element.  $\mu = \frac{(\Delta G^0 + \lambda)}{\sqrt{4\lambda_f k_B T}}$ ,<sup>1,2</sup> where  $\Delta G^0$  is the standard free energy difference of the reaction and  $\lambda$  is the total reorganization energy which is the sum of  $\lambda_f$  and  $\lambda_s$  corresponding to fast reorganization energy due to harmonic bond fluctuations and slow reorganization energy due to protein end-to-end distance fluctuations, respectively.  $\gamma = \sqrt{\frac{\lambda_s}{2\lambda_f N b^2}}$ , where  $N$  is the number of monomers of size  $b$ . The solution of the above equation is given by

$$P(t) = P(0) \exp\left(-\int_0^t k(R(t')) dt'\right). \quad (3)$$

The above equation when averaged over the distribution of  $R(t)$  yields the survival probability<sup>10</sup> of the unreacted electron donor state that survives up to time  $t$ . The latter is directly proportional to the intensity of transient absorption measured

in the experiment.<sup>4</sup> Carrying out the average yields

$$S(t) = \langle P(t) \rangle = P(0) \left\langle \exp \left( - \int_0^t k(R(t')) dt' \right) \right\rangle. \quad (4)$$

The stochastic evolution of the reaction coordinate associated with the end-to-end distance fluctuations in a protein backbone is presented in Sec. II A.

### A. Generalized Langevin equation for the end-to-end vector

The expression for the survival probability obtained above is similar to the one presented in Ref. 4. However, in Ref. 4 the time evolution of the reaction coordinate, the inter-segment distance  $x$ , was modelled as a particle in a one-dimensional harmonic potential driven by the fractional Gaussian noise. In the present work, the protein conformational fluctuations about the ground energetic state, occurring in a three-dimensional space, are parametrized by  $\mathbf{r}_n(t) = \mathbf{r}_n^0 + \mathbf{u}_n(t)$ , where  $\mathbf{r}_n^0$  is the position vector of the  $n$ th monomer in the energetic ground state and  $\mathbf{u}_n(t)$  is the deviation of the  $n$ th monomer from its ground state conformation. Protein conformation dynamics can, therefore, be effectively described by considering the stochastic dynamics of the end-to-end vector,  $\mathbf{R}(t) = \mathbf{r}_N(t) - \mathbf{r}_0(t) = \mathbf{R}^0 + \mathbf{u}_N(t) - \mathbf{u}_0(t)$ , of a protein backbone, where  $\mathbf{R}^0 = \mathbf{r}_N^0 - \mathbf{r}_0^0$  is the end-to-end vector of a protein chain in its energetic ground state and subscripts 0 and  $N$  label the first and last monomers, respectively. It is to be noted that the consideration of the end-to-end distance as opposed to the inter-segment distance  $\mathbf{R}_{nm}(t) = \mathbf{r}_n^0 + \mathbf{u}_n(t) - \mathbf{u}_m(t)$  as the reaction coordinate while simplifying the present analysis does not affect the quantitative results.<sup>6</sup>

The scalar component of the end-to-end vector,  $\mathbf{R}(t)$ , is related to the reaction coordinate,  $R(t)$ , through  $R(t) = \sqrt{\mathbf{R}(t) \cdot \mathbf{R}(t)}$ . Using the simplest Rouse-like dynamics for the harmonic deviations  $\mathbf{u}_n(t)$ , introduced earlier<sup>6</sup> to explain the two-point and four-point autocorrelations of the fluorescence lifetime fluctuations associated with the distance fluctuations of the protein flavin reductase,<sup>5</sup> the stochastic time evolution of the displacement vector is given by

$$\zeta \frac{\partial \mathbf{u}_n(t)}{\partial t} = k \frac{\partial^2 \mathbf{u}_n(t)}{\partial n^2} + \mathbf{f}_n(t). \quad (5)$$

The above equation is a force balance equation, where the first term is due to the dissipative force, the second term represents the force due to entropic elasticity arising from the chain connectivity, and the last term represents the random noise term. Here,  $\zeta$  is a friction coefficient,  $k = 3k_B T / b^2$  is an entropic spring constant and  $\mathbf{f}_n$  is a Gaussian white noise satisfying  $\langle \mathbf{f}_n(t) \mathbf{f}_m(t') \rangle = 2k_B T \zeta \delta_{nm} \delta(t - t')$ .

In what follows, we use the Markovian dynamics of protein normal modes to describe the non-Markovian dynamics of the reaction coordinate associated with protein distance fluctuations. Given that the two ends of the chain are free of external force, the displacement at the two ends should satisfy  $\partial \mathbf{u}_n / \partial n = 0$  at  $n = 0$  and  $n = N$ . In terms of the normal modes, therefore, the displacement vector is given by  $\mathbf{u}_n(t) = 2 \sum_{p=1}^{\infty} \mathbf{Q}_p(t) \cos(p\pi n / N) - \mathbf{R}^0$ , resulting in the following equation for the time evolution of the protein

normal modes:

$$\zeta_p \frac{\partial \mathbf{Q}_p(t)}{\partial t} = -k_p \mathbf{Q}_p(t) + \mathbf{F}_p(t), \quad (6)$$

where  $\zeta_p = 2N\zeta$  is the friction coefficient of the  $p$ th mode,  $k_p = 6p^2 \pi^2 k_B T / Nb^2$  is the entropic spring constant of the  $p$ th mode and  $\mathbf{f}_n(t) = 2 \sum_{p=1}^{\infty} \mathbf{F}_p(t) \cos(p\pi n / N)$ .<sup>11</sup>

From the above equation, the time-correlation function of the protein normal modes follows

$$\langle \mathbf{Q}_p(0) \cdot \mathbf{Q}_q(t) \rangle = \delta_{pq} \frac{Nb^2}{(p^2 + q^2)\pi^2} \exp(-p^2 t / \tau). \quad (7)$$

The above equation shows that each mode is uncorrelated with all other modes and relaxes as a single exponential with its own distinct relaxation time,  $\tau/p^2$ , where  $\tau = Nb^2 \zeta_p / 6\pi^2 k_B T$  is the longest relaxation time associated with the first normal mode. These features of the correlation function show that the fluctuations of the individual normal mode are governed by the Ornstein-Uhlenbeck process,<sup>12</sup> and are thereby Gaussian and Markovian in nature. Since the end-to-end vector is related to the sum of the normal modes,  $\mathbf{R}(t) = -4 \sum_{p=1, \text{ odd}} \mathbf{Q}_p(t)$ , the time correlation of distance fluctuations is given by

$$\rho(t) = 8 \sum_{p: \text{ odd}} \frac{Nb^2}{p^2 \pi^2} e^{-p^2 t / \tau}, \quad (8)$$

indicating that the end-to-end distance fluctuations are governed by the superimposed Ornstein-Uhlenbeck process and are therefore Gaussian and non-Markovian in nature.<sup>12</sup> As a result of the latter, the time evolution of the end-to-end vector is governed by the underdamped non-Markovian generalized Langevin equation with a memory kernel and the Gaussian colored noise given by<sup>6,13,14</sup>

$$\int_0^t dt' K(t - t') \frac{d\mathbf{R}(t')}{dt'} = -\frac{3k_B T}{Nb^2} \mathbf{R}(t) + \mathbf{f}(t), \quad (9)$$

where the mean and the variance of the Gaussian colored noise are given by  $\langle \mathbf{f}(t) \rangle = 0$  and  $\langle f_\alpha(0) f_\beta(t) \rangle = k_B T K(t) \delta_{\alpha\beta}$ , respectively, with  $K(t)$  being the friction kernel. Also, the first term on the right hand side represent the effective elastic force due to chain connectivity originating from the entropic contribution to the free energy,<sup>11</sup> given by  $F(\mathbf{R}) = \frac{3k_B T}{2Nb^2} \mathbf{R}^2$ , which is harmonic in nature. To obtain a closed form analytical expression for  $K(t)$ , the above equation can be multiplied with  $\mathbf{R}(0)$ , averaged, and Laplace transformed to yield

$$K(s) = \frac{3k_B T}{Nb^2} \frac{C(s)}{1 - sC(s)}, \quad (10)$$

where  $K(s) = \frac{3k_B T}{Nb^2} \int_0^\infty dt \exp(-st) K(t)$  is the Laplace transform of  $K(t)$  and  $C(s) = \rho(s) / \rho(0)$ . A closed form analytical expression for  $K(s)$  can be obtained by replacing the summation by integration in Eq. (8), Laplace transforming the resulting expression and substituting it in the above expression to yield

$$K(s) = \frac{3k_B T}{Nb^2} \sqrt{\frac{\tau}{s}} \left[ 1 - \frac{1}{\sqrt{s\tau}} \left[ \frac{\pi}{2} - \tan^{-1} \left( \frac{1}{\sqrt{s\tau}} \right) \right] \right] \left[ \frac{\pi}{2} - \tan^{-1} \left( \frac{1}{\sqrt{s\tau}} \right) \right]. \quad (11)$$

For times longer than the longest relaxation time,  $s\tau \ll 1$ , the above expression reduces to  $K(s) \approx \frac{k_B T}{Nb^2} \tau \approx N\zeta$ , which implies that the friction memory kernel is given by  $K(t) \approx \zeta_R \delta(t)$ , where  $\zeta_R = N\zeta$  is the total friction coefficient of the chain.<sup>11</sup> Since  $K(t) \propto \delta(t)$ , the Markovian limit is reassuringly recovered at long times.<sup>13,14</sup> In contrast, for times shorter than the longest relaxation time,  $s\tau \gg 1$ ,  $K(s) \approx \frac{k_B T}{Nb^2} \sqrt{\tau/s}$ , implying that  $K(t) \propto 1/\sqrt{t}$ .

In a previous work, the dynamics of inter-segment distance which effectively modulate the electron transfer reaction was described by considering the time evolution of a particle in a harmonic potential driven by the fractional Gaussian noise.<sup>4</sup> In this model, the effective friction coefficient was assumed to be given by  $K(t) = 2H(2H - 1)t^{2H-2}$ , where  $H$  is the Hurst index lying between 1/2 and 1. A good fit to experimental data was obtained by taking  $H = 3/4$ . However, no physical interpretation for this special choice, which yields  $K(t) \propto 1/\sqrt{t}$ , was provided. In the non-Markovian generalized Langevin equation approach used here, the colored Gaussian noise is fully described in terms of the microscopics of the non-Markovian distance fluctuations arising from the superposition of the Markovian fluctuations of the protein normal modes. The power law,  $t^{-1/2}$ , dependence of the friction kernel, observed experimentally,<sup>7</sup> therefore arises naturally. For times shorter than the longest relaxation time, the power law decay of the friction kernel is due to the non-Markovian distance fluctuations which at long times recovers the expected Markovian limit resulting in delta-function correlated white noise. The expression for the fractional Gaussian noise in Ref. 4, however, does not recover the expected limit of delta-function correlated white noise at long times.

## B. Survival probability of electron donor state

To obtain the expression for the probability distribution of  $\mathbf{R}(t)$ , the generalized Langevin equation can be transformed into the Smoluchowski equation by following the calculation presented in Appendix B. The resulting expression is

$$\frac{\partial P(\mathbf{R}, t)}{\partial t} = D(t) \left[ \frac{\partial}{\partial \mathbf{R}} \cdot \mathbf{R}P(\mathbf{R}, t) + \frac{Nb^2}{3} \frac{\partial^2}{\partial \mathbf{R}^2} P(\mathbf{R}, t) \right], \quad (12)$$

where  $D(t) = -\frac{\dot{C}(t)}{C(t)}$  is the time dependent diffusion coefficient and  $C(t)$  is the time correlation of the distance

fluctuations in a protein, given by

$$C(t) = \frac{\rho(t)}{\rho(0)} = \frac{8}{\pi^2} \sum_{p:odd} \frac{1}{p^2} \exp(-p^2 t/\tau). \quad (13)$$

If  $P(\mathbf{R}, t|\mathbf{R}_0, 0)$  represents the conditional probability that the end-to-end vector of a chain which was  $\mathbf{R}_0$  at time  $t = 0$  is  $\mathbf{R}$  at time  $t$  then this probability is obtained from the following Smoluchowski equation:

$$\begin{aligned} & \frac{\partial P(\mathbf{R}, t|\mathbf{R}_0, 0)}{\partial t} \\ &= D(t) \left[ \frac{\partial}{\partial \mathbf{R}} \cdot \{\mathbf{R}P(\mathbf{R}, t|\mathbf{R}_0, 0)\} + \frac{Nb^2}{3} \frac{\partial^2}{\partial \mathbf{R}^2} P(\mathbf{R}, t|\mathbf{R}_0, 0) \right] \end{aligned} \quad (14)$$

along with the initial condition<sup>11</sup>

$$P(\mathbf{R}, 0|\mathbf{R}_0, 0) = \delta(\mathbf{R} - \mathbf{R}_0). \quad (15)$$

The solution of the above equations, which is presented in Appendix C, yields the following Gaussian distribution:

$$\begin{aligned} P(\mathbf{R}, t|\mathbf{R}_0, 0) &= \left( \frac{3}{2\pi Nb^2 [1 - C^2(t)]} \right)^{3/2} \\ &\times \exp \left[ -\frac{3(\mathbf{R} - \mathbf{R}_0 C(t))^2}{2Nb^2 [1 - C^2(t)]} \right]. \end{aligned} \quad (16)$$

In the long time limit,  $t \rightarrow \infty$  when the correlation of the end-to-end vector at time  $t$  is completely uncorrelated with time  $t = 0$ ,  $C(t) = 0$  and the steady state distribution is given by

$$P_{ss}(\mathbf{R}) = \left( \frac{3}{2\pi Nb^2} \right)^{3/2} \exp \left[ -\frac{3\mathbf{R}^2}{2Nb^2} \right]. \quad (17)$$

Following Ref. 4, an approximate closed form expression for the survival probability can be obtained by expanding the exponential function on the right hand side of Eq. (4) to the second order in cumulants with stationary correlations, resulting in

$$\begin{aligned} S(t) &= \exp \left[ -\int_0^t dt' \langle k(R(t')) \rangle \right. \\ &\quad \left. + \int_0^t dt' (t - t') (\langle k(R(t')) k(R(0)) \rangle \right. \\ &\quad \left. - \langle k(R(t')) \rangle \langle k(R(0)) \rangle) \right]. \end{aligned} \quad (18)$$

Substituting the expression for the rate constant from Eq. (2) followed by integration over  $t'$  yields

$$\begin{aligned} S(t) &= \exp \left[ -t \alpha \beta \int_0^\infty dx x^2 \exp \left[ -x^2 \left( \gamma'^2 + \frac{3}{2} \right) + 2\mu \gamma' x \right] + \int_0^t dt' (t - t') \left\{ \alpha^2 \beta^2 \left( \frac{(1 - C^2(t'))^{-1/2}}{3C(t')} \right) \right. \right. \\ &\quad \left. \int_0^\infty dx \int_0^\infty dx_0 x x_0 \exp \left[ -(x^2 + x_0^2) \left( \gamma'^2 + \frac{3}{2(1 - C^2(t'))} \right) + 2\mu \gamma' (x + x_0) \right] \right. \\ &\quad \left. \times \sinh \left[ \frac{3C(t') x x_0}{(1 - C^2(t'))} \right] - \alpha^2 \beta^2 \left( \int_0^\infty dx x^2 \exp \left[ -x^2 \left( \gamma'^2 + \frac{3}{2} \right) + 2\mu \gamma' x \right] \right)^2 \right\} \right], \end{aligned} \quad (19)$$

where  $x = \frac{R}{N^{1/2}b}$ ,  $x_0 = \frac{R_0}{N^{1/2}b}$ ,  $\alpha = \left(\frac{J^2}{\hbar} \sqrt{\frac{\pi}{\lambda_f k_B T}}\right)$ ,  $\beta = 4\pi \left(\frac{3}{2\pi}\right)^{3/2} \exp(-\mu^2)$ ,  $\mu = \frac{(\Delta G^0 + \lambda)}{\sqrt{4\lambda_f k_B T}}$ , and  $\gamma' = \sqrt{\frac{\lambda_s}{2\lambda_f}}$ . The key steps involved in obtaining the above expression for the survival probability are summarized in Appendix D.

### III. RESULTS AND DISCUSSION

The expression for  $C(t)$  [Eq. (13)] provides a measure of the time-scale over which protein conformational fluctuations are correlated. The expression for  $S(t)$  [Eq. (19)], on the other hand, estimates the protein conformational dynamics modulated survival of the electron donor state up to time  $t$ . In Ref. 1, the time dependent diffusion coefficient  $D_p(t) = -\frac{\dot{C}_p(t)}{C_p(t)}$  had the same expression as here [Eq. (12)], where  $C_p(t)$  was the protein relaxation function. However, since protein conformational fluctuations were not explicitly included in Ref. 1,  $C_p(t)$  was considered as an empirical function, the functional form of  $C_p(t)$  which was obtained by fitting a tri-exponential function, with three distinct relaxation times as the fitting parameters, to the transient absorption signal at 280 nm. In the present work,  $C(t)$ , which has the same physical interpretation as  $C_p(t)$ , is not an empirical function but derived from the non-Markovian dynamics of protein distance fluctuations. The multiple exponential decay of  $C(t)$  which corresponds to the multiple relaxation times,  $\tau_p = \tau/p^2$ , over which protein normal modes relax naturally explain the multi-exponential empirical form of  $C_p(t)$  which was necessary to obtain a good fit with the transient absorption signal at 280 nm. It also explains the microscopic origins of the non-exponential decay of the experimental data in terms of the multiple time scales over which protein normal modes relax.

Data points in Fig. 1 correspond to the temporal decay of the transient absorption change at 280 nm due to protein conformational fluctuations which are invariant in different mutants leading to data collapse. The solid line in Fig. 1 shows the fitting of  $C(t)$  [Eq. (13)] with the transient absorption sig-

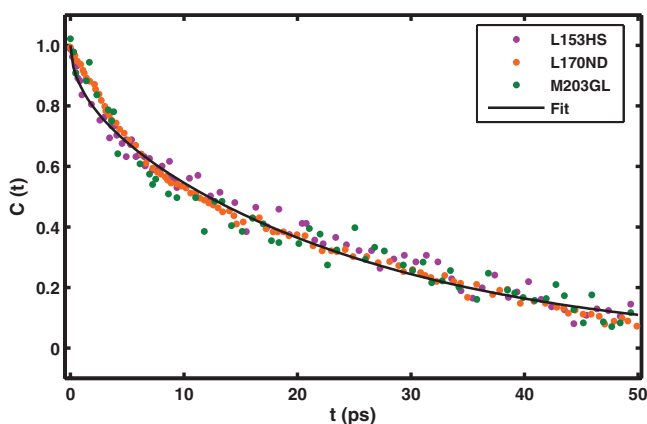


FIG. 1. The temporal decay of the transient absorbance change at 280 nm due to protein conformational fluctuations as measured in experiment<sup>1</sup> is compared with the end-to-end distance correlation of the protein backbone  $C(t)$  [Eq. (13)]. The solid line represent theoretical fit to experimental data for three different mutants of *Rhodobacter sphaeroides*, which yields the longest relaxation time corresponding to the first mode as  $\tau = 25$  ps.

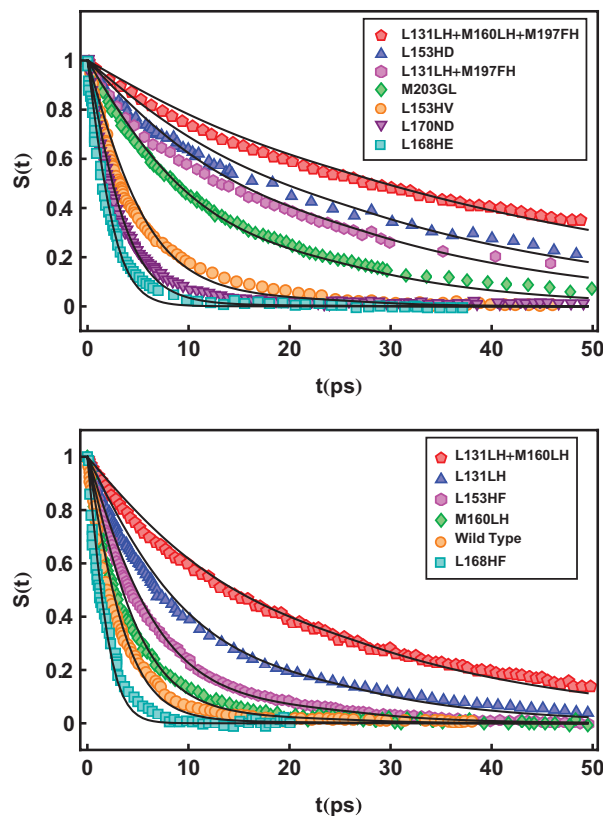


FIG. 2. The temporal decay of the transient absorbance change at 930 nm measured in experiment<sup>1</sup> is compared with the theoretical expression for survival probability  $S(t)$  [Eq. (19)] for wild type and twelve different mutants [seven (top) and six (bottom)] of *Rhodobacter sphaeroides*. Solid lines represent theoretical fit to the experimental data for the fitting parameters  $J = 40 \text{ cm}^{-1}$ ,  $\lambda_f = 350 \text{ meV}$ ,  $\lambda_s = 90 \text{ meV}$ ,  $T = 300 \text{ K}$ , and  $\tau = 25 \text{ ps}$ . While the standard free energy difference of wild type is taken to be  $\Delta G_{wt}^0 = -172 \text{ meV}$ , the fitting to different mutants is obtained by merely changing the relative free energy, tabulated in Table I as  $\Delta\Delta G_a^0$ .

nal at 280 nm which only requires one fitting parameter—the longest relaxation time associated with the first mode,  $\tau$ —as it fixes the relaxation time for all the higher modes through  $\tau_p = \tau/p^2$ . The good fitting is obtained for  $\tau = 25$  ps which fixes the value of  $C(t)$  in Eq. (19) for the survival probability,  $S(t)$ .

The solid lines in Fig. 2 show the fitting of the survival probability  $S(t)$ , evaluated numerically from Eq. (19), with the transient absorption signal at 930 nm. For the wild type reaction center the fitting parameters are  $\Delta G_{wt}^0 = -172 \text{ meV}$ ,  $J = 40 \text{ cm}^{-1}$ ,  $\lambda_f = 350 \text{ meV}$ ,  $\lambda_s = 90 \text{ meV}$ ,  $\tau = 25 \text{ ps}$ , and  $T = 300 \text{ K}$ . Keeping all these parameter fixed, the transient absorption signal at 930 nm for different mutants can be fitted by merely varying the standard free energy difference  $\Delta G_{mut}^0$  for different mutants with respect to the wild type reaction center, represented by the relative free energy difference,  $\Delta\Delta G^0 = \Delta G_{mut}^0 - \Delta G_{wt}^0$ . Table I shows the fitting parameters for the relative free energy difference  $\Delta\Delta G^0$  for different mutants, where the subscripts  $a, b, c$  correspond to the fitting parameters used in the present study, Refs. 1 and 4, respectively. In Ref. 1, where protein conformational fluctuations were not explicitly included in the model, the fitting parameters used were  $\Delta G^0 = -200 \text{ meV}$  (wild type),  $J = 39 \text{ cm}^{-1}$ ,  $\lambda_f = 280 \text{ meV}$ ,  $\lambda_s = 70 \text{ meV}$ , and  $T = 300 \text{ K}$ .

TABLE I. Comparison of the fitting parameters for the relative free energy for different mutants,  $\Delta\Delta G_{a,b,c}^0$ . The subscript  $a, b, c$  correspond to the fitting estimates for the present work, Refs. 1 and 4, respectively. In Ref. 4, good fitting has been obtained by additionally varying the relaxation time for the inter-segment distance fluctuations,  $\tau$ , the values of which are denoted within the square brackets.

| Species              | $\Delta\Delta G_a^0$<br>(meV) | $\Delta\Delta G_b^0$<br>(meV) | $\Delta\Delta G_c^0[\tau(ps)]$<br>(meV) |
|----------------------|-------------------------------|-------------------------------|---|
| L131LH+M160LH+M197FH | 152                           | 180                           | 155 [210]                               |
| L153HD               | 131                           | 148                           | 131 [190]                               |
| L131LH+M197FH        | 118                           | 140                           | 118 [185]                               |
| L131LH+M160LH        | 117                           | 136                           | 117 [180]                               |
| M203GL               | 90                            | 105                           | 93 [165]                                |
| L131LH               | 84                            | 99                            | 85 [154]                                |
| L153HF               | 52                            | 57                            | 50 [89]                                 |
| L153HV               | 37                            | 28                            | 26 [55]                                 |
| M160LH               | 27                            | 27                            | 25 [50]                                 |
| Wild type            | 0                             | 0                             | 0 [40]                                  |
| L170ND               | -1                            | -7                            | -0.7 [31]                               |
| L168HE               | -40                           | -48                           | -44 [21]                                |
| L168HF               | -68                           | -75                           | -60 [6]                                 |

In Ref. 4, on the other hand, where protein conformational fluctuations were included by considering the stochastic dynamics of a particle in a harmonic potential driven by the Gaussian fractional noise, the best fitting was obtained by considering the same fitting parameters [ $J, \lambda_f, \lambda_s$ , and  $T$ ] as in Ref. 1. However, in contrast to the present work and Ref. 1, the value of the protein relaxation time,  $\tau$ , was not obtained by fitting the theoretical curve with the signal at 280 nm, but by considering  $\tau$  as an additional fitting parameter. In Table I, the values of these additional fitting parameters [ $\tau$ ] are specified within the square brackets against  $\Delta\Delta G_c^0$  values for each mutant. Since data collapse for the signal at 280 nm for different mutants shows that protein conformational fluctuations are insensitive in different mutants and decays as a single non-exponential curve [Ref. 1], it is not clear why different values of the protein relaxation times are needed to obtain fitting for 930 nm signal for different mutants. One possible reason for this could be that the fractional Gaussian noise in Ref. 4 does not recover the expected limit of delta function correlated white noise at long times<sup>14</sup> and only provides a reasonable description for times shorter than the longest relaxation time of a protein.

The relative free energy difference for different mutants,  $\Delta\Delta G_{P/P^+}^0$  can be measured electrochemically, where  $P/P^+$  is the midpoint potential of each mutant and  $P$  is the initial electron donor.<sup>1,8</sup> The open circles in Fig. 3 represent the experimental estimates for  $\Delta\Delta G_{P/P^+}^0$  for five different mutants. These values are compared with the theoretical fitting estimates,  $\Delta\Delta G_{fit}^0$ , given in Table I corresponding to the present work and diffusion-reaction model of Ref. 1. Figure 3 shows that the theoretical estimates of the present model,  $\Delta\Delta G_a^0$  [squares] compare well with the theoretical estimates of the diffusion-reaction model,<sup>1</sup>  $\Delta\Delta G_b^0$  [triangles] and experimental estimates,  $\Delta\Delta G_{P/P^+}^0$  [circles] in Ref. 8.

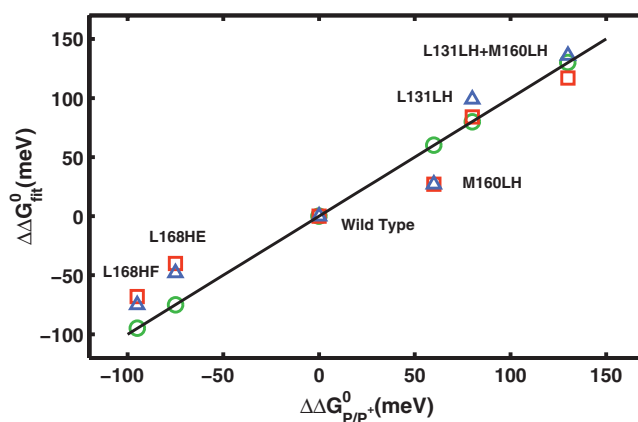


FIG. 3. Comparison of the theoretical estimates of the relative free energy difference,  $\Delta\Delta G_{a,b}^0$ , tabulated in Table I for the present study,  $\Delta\Delta G_a^0$  [squares], and the diffusion-reaction model,<sup>1</sup>  $\Delta\Delta G_b^0$  [triangles], with the experimental estimates  $\Delta\Delta G_{P/P^+}^0$  [circles] obtained using electrochemical measurements in Ref. 8 for five different mutants of *Rhodobacter sphaeroides*. The solid line is a guide to the eye.

#### IV. SUMMARY AND CONCLUSION

In this work, we have used a non-Markovian generalized Langevin equation approach to describe the stochastic dynamics of the reaction coordinate associated with protein distance fluctuations, which effectively modulates the electron transfer kinetics in early stage photosynthesis. The non-Markovian generalized Langevin equation description includes a memory kernel and colored Gaussian noise, both of which are completely described in terms of the microscopics of the protein normal mode fluctuations. This model yields an analytical expression for protein distance fluctuations,  $C(t)$  as a superposition of the protein normal modes relaxation with each mode decaying with its own relaxation time, resulting in multiple time scales of relaxation.  $C(t)$  provides excellent fit to the 280 nm signal associated with the protein conformational relaxation and yields the relaxation time of the first normal mode through which the relaxation time of all the higher modes can be obtained. The non-exponential relaxation of the latter can be understood in terms of the multiple time scales of relaxation of the normal modes. The harmonic potential assumed in Ref. 1 also finds its microscopic meaning in terms of the conformational entropy due to chain connectivity. The expression for the survival probability for electron donor state, on the other hand, provides excellent fits to the transient absorption signal at 930 nm, using the same  $C(t)$  obtained by fitting the 280 nm signal, for different mutants in the reaction center just by varying the driving force of the reaction relative to the wild type. The non-exponential decay of the latter is due to dynamic disorder in the electron transfer reaction pathway because of protein conformational fluctuations that occur on time scales slower than or comparable to the electron transfer reaction. The theoretical estimates for the relative driving force for five mutants are in reasonably good agreement with the experimental estimates obtained using electrochemical measurements.

The non-Markovian Langevin equation approach used here has earlier<sup>6</sup> provided excellent fits to the experimental

data measuring the two-point and four-point autocorrelations of the fluorescence lifetime fluctuations associated with the distance fluctuations of the protein flavin reductase over five decades in time and has also demonstrated a symmetry of these functions observed experimentally.<sup>5</sup> Given that the same model provides accurate fits to the transient absorbance signals for protein dynamics modulated electron transfer kinetics, explains the microscopic origin for the non-exponential decay of these signals, clarifies in terms of the protein normal mode fluctuations why the consideration of a tri-exponential empirical form for  $C_p(t)$  and a harmonic potential for protein distance fluctuations in Ref. 1 were sufficient to recover the experimental results, shows that several universal aspects of protein conformational fluctuations can be captured by the non-Markovian Langevin equation approach for distance fluctuations used here.

## ACKNOWLEDGMENTS

P.K. acknowledges the financial support from the University Grants Commission (UGC), Government of India.

## APPENDIX A: PROTEIN DYNAMICS MODULATED ELECTRON TRANSFER RATE CONSTANT

In Sumi-Marcus model, the electron transfer kinetics in a viscous solvent has been described in terms of the fast and slow reaction coordinates.<sup>2,3</sup> When the electron transfer kinetics is modulated by the conformational dynamics of a protein backbone, then the potential energy surface of reactants and products along the fast and slow reaction coordinates<sup>1</sup> can be given by

$$V^r(q, R) = \frac{1}{2}k_f q^2 + \frac{1}{2}k_s R^2, \quad (\text{A1})$$

$$V^p(q, R) = \frac{1}{2}k_f(q - q_0)^2 + \frac{1}{2}k_s(R - R_0)^2 + \Delta G^0, \quad (\text{A2})$$

where  $q$  and  $R$  are the respective fast and slow reaction coordinates associated with the harmonic fluctuations of the effective bond distance and end-to-end distance of a protein chain with  $k_f = k_B T/b^2$  and  $k_s = k_B T/Nb^2$  being the respective entropic spring constants.<sup>11</sup>  $q_0$  and  $R_0$  are the equilibrium values of  $q$  and  $R$ , respectively, and  $\Delta G^0$  is the standard free energy difference between the reactants and products. The fast and slow components of the total reorganizational energy  $\lambda$  are given by  $\lambda_f = k_f q_0^2/2$  and  $\lambda_s = k_s R_0^2/2$ , respectively, such that  $\lambda = \lambda_s + \lambda_f$ .<sup>1,2</sup> In Ref. 1, where the protein conformational fluctuations are not explicitly included, the functional form of the potential,  $V_p(x)$ , associated with the slow reaction coordinate was not specified, but was assumed to be harmonic in nature. In the present work, the probability distribution of the effective bond distance and the end-to-end distance follow the Gaussian distributions.<sup>6,11</sup> The quadratic dependence of the effective bond distance and end-to-end distance, associated with the fast and slow reaction coordinates, therefore, appears naturally.

The potential energy surfaces of reactants and products intersect when  $V^r(q^\dagger, R) = V^p(q^\dagger, R)$ ,<sup>2</sup> yielding

$$q^\dagger = \frac{(\Delta G^0 + \lambda) - k_s R R_0}{k_f q_0}. \quad (\text{A3})$$

Given that the electron transfer rate is given by  $k(R) = \nu_f \exp(-\Delta G^\ddagger(R)/k_B T)$ , where  $\nu_f = \frac{J^2}{\hbar} \sqrt{\frac{\pi}{\lambda_f k_B T}}$  is the frequency factor and  $\Delta G^\ddagger(R) = V^r(q^\dagger, R) - V^r(0, R)$  is the free energy difference, Eqs. (A1) and (A3) yield<sup>2</sup>

$$\Delta G^\ddagger(R) = \frac{1}{2}k_a q^{\ddagger 2} = \frac{\left(\Delta G^0 + \lambda - \sqrt{\frac{2\lambda_s k_B T}{Nb^2}} R\right)^2}{4\lambda_f} \quad (\text{A4})$$

resulting in

$$k(R) = \left(\frac{J^2}{\hbar} \sqrt{\frac{\pi}{\lambda_f k_B T}}\right) \exp[-(\mu - \gamma R)^2], \quad (\text{A5})$$

where  $\mu = \frac{(\Delta G^0 + \lambda)}{\sqrt{4\lambda_f k_B T}}$  and  $\gamma = \sqrt{\frac{\lambda_s}{2\lambda_f Nb^2}}$ . The above expression is the same as Eq. (2). It is to be noted that in real systems the electronic coupling matrix  $J$  and the fast reorganization energy  $\lambda_f$  can depend on the distance and orientation of the donor-acceptor pair.<sup>15,16</sup> Here, the presence of protein conformational fluctuations which effectively modulate electron transfer kinetics require the presence of slow reaction coordinate along with the fast one. This makes the present analysis complex compared to earlier works. Given the complexity of the present calculation, we have assumed  $J$  and  $\lambda_f$  to be constant.

## APPENDIX B: DERIVATION OF THE SMOLUCHOWSKI EQUATION

The expression for the probability distribution of  $\mathbf{R}(t)$  can be obtained by transforming the generalized Langevin equation into the Smoluchowski equation. The details of the method are given in Refs. 17–21. Here we outline the key steps relevant to the present calculation.

The Laplace transform of the generalized Langevin equation [Eq. (9)] yields

$$\mathbf{R}(s) = \mathbf{R}(0) C(s) + \mathbf{f}(s) \phi(s) \frac{Nb^2}{3k_B T}, \quad (\text{B1})$$

where  $C(s) = \frac{K(s)}{sK(s) + \frac{3k_B T}{Nb^2}}$  and  $\phi(s) = 1 - sC(s)$ .

Equation (B1) can be Laplace inverted to yield

$$\mathbf{R}(t) = \mathbf{R}(0) C(t) + \frac{Nb^2}{3k_B T} \int_0^t dt' \phi(t-t') \mathbf{f}(t'). \quad (\text{B2})$$

The time derivative of Eq. (B2) yields

$$\dot{\mathbf{R}}(t) = -D(t) \mathbf{R}(t) + \frac{Nb^2}{3k_B T} C(t) \frac{d}{dt} \int_0^t dt' \frac{\phi(t-t')}{C(t)} \mathbf{f}(t'), \quad (\text{B3})$$

where  $D(t) = -\frac{\dot{C}(t)}{C(t)}$ .

Defining  $P(\mathbf{R}, t) = \langle \delta(\mathbf{R}(t) - \mathbf{R}) \rangle$  and differentiating it with respect to  $t$  yields

$$\frac{\partial P(\mathbf{R}, t)}{\partial t} = -\frac{\partial}{\partial \mathbf{R}} \langle \delta(\mathbf{R}(t) - \mathbf{R}) \dot{\mathbf{R}}(t) \rangle. \quad (\text{B4})$$

Substitution of Eq. (B3) into Eq. (B4) results in

$$\frac{\partial P(\mathbf{R}, t)}{\partial t} = D(t) \frac{\partial}{\partial \mathbf{R}} \cdot \mathbf{R} P(\mathbf{R}, t) - \frac{Nb^2}{3k_B T} \frac{\partial}{\partial \mathbf{R}} \langle \delta(\mathbf{R}(t) - \mathbf{R}) \bar{\mathbf{f}}(t) \rangle, \quad (\text{B5})$$

where  $\bar{\mathbf{f}}(t) = C(t) \frac{d}{dt} \int_0^t dt' \frac{\phi(t-t')}{C(t')} \mathbf{f}(t')$ .

Using Novikov's theorem in Eq. (B5)

$$\langle \delta(\mathbf{R}(t) - \mathbf{R}) \bar{\mathbf{f}}(t) \rangle = - \frac{\partial}{\partial \mathbf{R}} \int_0^t dt' \langle \bar{\mathbf{f}}(t) \bar{\mathbf{f}}(t') \rangle \left\langle \delta(\mathbf{R}(t) - \mathbf{R}) \frac{\delta \mathbf{R}(t)}{\delta \bar{\mathbf{f}}(t)} \right\rangle. \quad (\text{B6})$$

The functional derivative in Eq. (B6) is obtained using the solution of Eq. (B3), resulting in

$$\frac{\delta \mathbf{R}(t)}{\delta \bar{\mathbf{f}}(t)} = \frac{Nb^2}{3k_B T} \exp \left[ - \int_{t'}^t dt_1 D(t_1) \right]. \quad (\text{B7})$$

From Eqs. (B5)–(B7), the corresponding Smoluchowski equation is given by

$$\frac{\partial P(\mathbf{R}, t)}{\partial t} = D(t) \frac{\partial}{\partial \mathbf{R}} \cdot \mathbf{R} P(\mathbf{R}, t) + \left( \frac{Nb^2}{3k_B T} \right)^2 \frac{\partial^2}{\partial \mathbf{R}^2} P(\mathbf{R}, t) A(t), \quad (\text{B8})$$

where  $A(t) = \int_0^t dt' \langle \bar{\mathbf{f}}(t) \bar{\mathbf{f}}(t') \rangle \exp \left[ - \int_{t'}^t dt_1 D(t_1) \right]$ .

The explicit expression for  $\bar{\mathbf{f}}(t)$  when substituted in the expression for  $A(t)$  yields

$$A(t) = \frac{1}{2} C^2(t) \frac{d}{dt} \frac{1}{C^2(t)} k_B T \int_0^t dt_1 \times \int_0^{t_1} dt_2 \phi(t-t_1) \phi(t-t_2) K(t_2-t_1). \quad (\text{B9})$$

Following Fox,<sup>21</sup> the double integral part of Eq. (B9) can be solved using the method of double Laplace transform, resulting in

$$\frac{3k_B T}{Nb^2} [1 - C^2(t)]. \quad (\text{B10})$$

Substituting the above expression into Eq. (B9) yields

$$A(t) = \frac{3(k_B T)^2}{Nb^2} D(t). \quad (\text{B11})$$

Substitution of Eq. (B11) into Eq. (B8) results in Eq. (12).

### APPENDIX C: SOLUTION OF THE SMOLUCHOWSKI EQUATION

The Fourier transform of Eq. (12) yields

$$\frac{dY(\mathbf{k}, t | \mathbf{R}_0, 0)}{dt} = \left[ -D(t) \mathbf{k} \frac{\partial}{\partial \mathbf{k}} - \frac{Nb^2}{3} D(t) \mathbf{k}^2 \right] Y(\mathbf{k}, t | \mathbf{R}_0, 0), \quad (\text{C1})$$

where

$$Y(\mathbf{k}, t | \mathbf{R}_0, 0) = \int_{-\infty}^{\infty} d\mathbf{R} P(\mathbf{R}, t | \mathbf{R}_0, 0) e^{-i\mathbf{k} \cdot \mathbf{R}}. \quad (\text{C2})$$

Equation (C1) can be solved by the method of characteristics,<sup>12,22</sup> which yields

$$Y(\mathbf{k}, t | \mathbf{R}_0, 0) = \exp \left[ - \frac{Nb^2 \mathbf{k}^2}{6} \right] \Omega(\mathbf{k} C(t)), \quad (\text{C3})$$

where  $\Omega$  is an unknown function, the form of which can be determined in such a way that the initial conditions are satisfied.

Using the initial condition,  $P(\mathbf{R}, 0 | \mathbf{R}_0, 0) = \delta(\mathbf{R} - \mathbf{R}_0)$ , in Eq. (C2) yields

$$Y(\mathbf{k}, 0 | \mathbf{R}_0, 0) = e^{-i\mathbf{k} \cdot \mathbf{R}_0} = \exp \left[ - \frac{Nb^2 \mathbf{k}^2}{6} \right] \Omega(\mathbf{k}), \quad (\text{C4})$$

resulting in

$$\Omega(\mathbf{k}) = \exp \left[ -i\mathbf{k} \cdot \mathbf{R}_0 + \frac{Nb^2 \mathbf{k}^2}{6} \right]. \quad (\text{C5})$$

Replacing  $\mathbf{k}$  by  $\mathbf{k} C(t)$  in Eq. (C5) results

$$\Omega(\mathbf{k} C(t)) = \exp \left[ -i\mathbf{k} \cdot \mathbf{R}_0 C(t) + \frac{Nb^2 \mathbf{k}^2 C^2(t)}{6} \right]. \quad (\text{C6})$$

Substitution of Eq. (C6) into Eq. (C3) yields

$$Y(\mathbf{k}, t | \mathbf{R}_0, 0) = \exp[-i\mathbf{k} \cdot \mathbf{R}_0 C(t)] \times \exp \left[ - \frac{Nb^2 \mathbf{k}^2}{6} \{1 - C^2(t)\} \right]. \quad (\text{C7})$$

The inverse Fourier transform of Eq. (C7) yields the solution of the Smoluchowski equation, given by Eq. (16).

### APPENDIX D: DERIVATION OF THE TIME DEPENDENT SURVIVAL PROBABILITY

The calculation of the survival probability requires the explicit expressions for the rate-rate correlation functions in Eq. (18) which can be evaluated using Eqs. (2), (16), and (17).

$$\begin{aligned} \langle k(R(t)) \rangle &= \langle k(R(0)) \rangle \\ &= \int_{-\infty}^{\infty} d\mathbf{R} k(R) P_{ss}(\mathbf{R}) \\ &= \left( \frac{J^2}{\hbar} \sqrt{\frac{\pi}{\lambda_f k_B T}} \right) \left( \frac{3}{2\pi Nb^2} \right)^{3/2} 4\pi \exp(-\mu^2) \\ &\quad \times \int_0^{\infty} dR R^2 \exp \left[ -R^2 \left( \gamma^2 + \frac{3}{2Nb^2} \right) + 2\mu\gamma R \right]. \end{aligned} \quad (\text{D1})$$

$$\begin{aligned}
\langle k(R(t))k(R(0)) \rangle &= \int_{-\infty}^{\infty} d\mathbf{R} \int_{-\infty}^{\infty} d\mathbf{R}_0 k(R) P(\mathbf{R}, t | \mathbf{R}_0, 0) k(R_0) P_{ss}(\mathbf{R}_0) \\
&= \left( \frac{J^2}{\hbar} \sqrt{\frac{\pi}{\lambda_f k_B T}} \right)^2 \left( \frac{3}{2\pi N b^2} \right)^3 \left( \frac{1}{1 - C^2(t)} \right)^{3/2} 8\pi^2 \exp(-2\mu^2) \\
&\quad \int_0^{\infty} dR \int_0^{\infty} dR_0 R^2 R_0^2 \exp \left[ -(R^2 + R_0^2) \left( \gamma^2 + \frac{3}{2 N b^2 (1 - C^2(t))} \right) + 2\mu \gamma (R + R_0) \right] \\
&\quad \int_0^{\pi} \exp \left[ \frac{3 C(t) R R_0 \cos \theta}{N b^2 (1 - C^2(t))} \right] \sin \theta d\theta \\
&= \left( \frac{J^2}{\hbar} \sqrt{\frac{\pi}{\lambda_f k_B T}} \right)^2 \left( \frac{3}{2\pi N b^2} \right)^3 \frac{N b^2}{3 C(t) (1 - C^2(t))^{1/2}} 16\pi^2 \exp(-2\mu^2) \\
&\quad \int_0^{\infty} dR \int_0^{\infty} dR_0 R R_0 \exp \left[ -(R^2 + R_0^2) \left( \gamma^2 + \frac{3}{2 N b^2 (1 - C^2(t))} \right) + 2\mu \gamma (R + R_0) \right] \\
&\quad \times \sinh \left[ \frac{3 C(t) R R_0}{N b^2 (1 - C^2(t))} \right]. \tag{D2}
\end{aligned}$$

Substituting Eqs. (D1) and (D2) into Eq. (18) the expression of the survival probability becomes

$$\begin{aligned}
S(t) &= \exp \left[ -t \alpha \beta \left( \frac{1}{N b^2} \right)^{3/2} \int_0^{\infty} dR R^2 \exp \left[ -R^2 \left( \gamma^2 + \frac{3}{2 N b^2} \right) + 2\mu \gamma R \right] + \int_0^t dt' (t - t') \left\{ \alpha^2 \beta^2 \left( \frac{1}{N b^2} \right)^2 \right. \right. \\
&\quad \left. \left( \frac{(1 - C^2(t))^{-1/2}}{3 C(t)} \right) \int_0^{\infty} dR \int_0^{\infty} dR_0 R R_0 \exp \left[ -(R^2 + R_0^2) \left( \gamma^2 + \frac{3}{2 N b^2 (1 - C^2(t))} \right) + 2\mu \gamma (R + R_0) \right] \right. \\
&\quad \left. \times \sinh \left[ \frac{3 C(t) R R_0}{N b^2 (1 - C^2(t))} \right] - \alpha^2 \beta^2 \left( \frac{1}{N b^2} \right)^3 \left( \int_0^{\infty} dR R^2 \exp \left[ -R^2 \left( \gamma^2 + \frac{3}{2 N b^2} \right) + 2\mu \gamma R \right] \right)^2 \right\} \right], \tag{D3}
\end{aligned}$$

where  $\alpha = \left( \frac{J^2}{\hbar} \sqrt{\frac{\pi}{\lambda_f k_B T}} \right)$ ,  $\beta = 4\pi \left( \frac{3}{2\pi} \right)^{3/2} \exp(-\mu^2)$ ,  $\mu = \frac{(\Delta G^0 + \lambda)}{\sqrt{4\lambda_f k_B T}}$  and  $\gamma = \sqrt{\frac{\lambda_s}{2 N b^2 \lambda_f}}$ .

Equation (D3) can be made dimensionless by considering  $\frac{R}{N^{1/2} b} = x$  and  $\frac{R_0}{N^{1/2} b} = x_0$  and the final expression of the survival probability is given by Eq. (19).

- <sup>1</sup>H. Wang, S. Lin, J. P. Allen, J. C. Williams, S. Blankert, C. Laser, and N. W. Woodbury, *Science* **316**, 747 (2007).  
<sup>2</sup>H. Sumi and R. A. Marcus, *J. Chem. Phys.* **84**, 4272 (1986).  
<sup>3</sup>A. Okada, *J. Phys. Chem. A* **104**, 7744 (2000).  
<sup>4</sup>S. Chaudhury and B. J. Cherayil, *J. Chem. Phys.* **127**, 145103 (2007).  
<sup>5</sup>S. C. Kou and X. S. Xie, *Phys. Rev. Lett.* **93**, 180603 (2004).  
<sup>6</sup>A. Dua and R. Adhikari, *J. Stat. Mech.* **2011**, P04017.  
<sup>7</sup>W. Min, G. Luo, B. J. Cherayil, S. C. Kou, and X. S. Xie, *Phys. Rev. Lett.* **94**, 198302 (2005).  
<sup>8</sup>X. Lin, H. A. Murchison, V. Nagarajan, W. W. Parson, J. P. Allen, and J. C. Williams, *Proc. Natl. Acad. Sci. U.S.A.* **91**, 10265 (1994).

- <sup>9</sup>R. Zwanzig, *Acc. Chem. Res.* **23**, 148 (1990); *J. Chem. Phys.* **97**, 3587 (1992).  
<sup>10</sup>S. Yang and J. Cao, *J. Chem. Phys.* **117**, 10996 (2002).  
<sup>11</sup>M. Doi and S. Edwards, *The Theory of Polymer Dynamics* (Clarendon, Oxford, 1986).  
<sup>12</sup>N. G. V. Kampen, *Stochastic Processes in Physics and Chemistry* (North-Holland, Amsterdam, 1981).  
<sup>13</sup>R. F. Fox, *Phys. Rep.* **48**, 179 (1978).  
<sup>14</sup>R. Zwanzig, *Nonequilibrium Statistical Mechanics* (Oxford University Press, 2001).  
<sup>15</sup>T. R. Prytkova, I. V. Kurnikov, and D. N. Beratan, *Science* **315**, 622 (2007).  
<sup>16</sup>H. Oberhofer and J. Blumberger, *Angew. Chem., Int. Ed.* **49**, 3631 (2010).  
<sup>17</sup>S. Chaudhury and B. J. Cherayil, *J. Chem. Phys.* **125**, 024904 (2006).  
<sup>18</sup>S. Okuyama and D. Oxtoby, *J. Chem. Phys.* **84**, 5824 (1986).  
<sup>19</sup>M. San Miguel and M. Sancho, *J. Stat. Phys.* **22**, 605 (1980).  
<sup>20</sup>P. Hanggi, *Z. Phys. B* **31**, 407 (1978).  
<sup>21</sup>R. F. Fox, *J. Math. Phys.* **18**, 2331 (1977).  
<sup>22</sup>D. Zwillinger, *Handbook of Differential Equations* (Academic, San Diego, CA, 1989).